

**CARBON MONOXIDE CHEMISORPTION AND DISPROPORTIONATION ON THIN PALLADIUM LAYERS, SUPPORTED BY NIOBIUM AND NIOBIUM PENTOXIDE**

Jan PLŠEK<sup>1,\*</sup>, Vladimír NIKOLAJENKO<sup>2</sup>, Michel Malick THIAM<sup>3</sup> and Zlatko KNOR<sup>4</sup>

*J. Heyrovský Institute of Physical Chemistry, Academy of Sciences of the Czech Republic, Dolejškova 3, 182 23 Prague 8, Czech Republic; e-mail: <sup>1</sup> jan.plsek@jh-inst.cas.cz,*

*<sup>2</sup> nikolajenko@seznam.cz, <sup>3</sup> thiamm@postman.riken.go.jp, <sup>4</sup> zlatko.knor@jh-inst.cas.cz*

Received June 30, 2003

Accepted July 28, 2003

Thermally programmed desorption technique has been applied to the investigation of "virgin" and repeated adsorption of carbon monoxide on Pd/Nb and Pd/Nb<sub>2</sub>O<sub>5</sub>/Nb systems. The desorbed products of the CO interaction with these surfaces, CO and CO<sub>2</sub>, were monitored with a quadrupole mass spectrometer. On the basis of presented results some of the observed differences between the metal- and oxide-supported active metal (Pd) have been ascribed to the morphological rather than to chemical (electronic) effects in these systems. The different excess kinetic energy dissipation of Pd atoms colliding with metallic or oxidic surface is considered to influence the initial growth of the Pd layer, resulting afterwards in a different morphology of the final Pd layers.

**Keywords:** Thermally programmed desorption; Energy dissipation; Carbon monoxide; Adsorption; Disproportionation; Metallic supports; Oxidic supports; Morphology of vacuum deposited layers; Early transition metals; Late transition metals.

Carbon monoxide oxidation on oxide-supported metals ranks among catalytic reactions of great practical importance, particularly with respect to the air pollution problems. Consequently, interactions of carbon monoxide with and/or on solid surfaces was in the past a subject of many experimental and theoretical studies. Both model and commercial-type catalysts have been so far investigated by various methods. However, some experimental findings are not fully understood yet, *e.g.* the detailed role of the support in the surface interaction itself. The surface of the support can be considered: (i) as an inert matrix (preventing only the highly dispersed metallic catalyst from sintering); (ii) as a partly active component of a catalyst, representing the so called "collection zones" around the individual metallic 2D or 3D islands<sup>1,2</sup>; (iii) as an active component of a bifunctional catalyst; (iv) as influ-

encing the electronic and/or geometric structure of metallic particles during their preparation.

Some of the above listed problems are attempted to be elucidated in this study, namely, the influence of the chemical nature of the support (Nb and Nb<sub>2</sub>O<sub>5</sub>) and of the overlayer (Pd) thickness on its chemisorption activity considering the reactant molecules themselves (CO) as probes of catalyst surface properties. This paper represents an extension of our preliminary study of the same systems<sup>3</sup>. Thermally programmed desorption (TPD) and thermally programmed reaction (TPR) techniques were mainly used and conclusions, drawn from these experiments, were in some cases supported by independent XPS measurements<sup>4</sup>.

Our interest in Pd/Nb and Pd/Nb<sub>2</sub>O<sub>5</sub> systems was raised by earlier studies of thin layers of late transition metals (Pd, Pt) deposited on the surfaces of early transition metals (Nb, Ta, W, Mo). Submonolayers of, *e.g.*, palladium exhibited electronic structure and accordingly also chemisorption activity, resembling those of noble metal surfaces (see citations in refs<sup>3,5,6</sup>). On the other hand, thicker Pd layers already exhibited ordinary palladium properties. Thin niobium pentoxide interlayers in our experiments were expected to change the geometric structure of the niobium surface prior to the palladium deposition. This should thus prevent the formation of a pseudomorphic structure in the case of the deposited palladium submonolayer. The formation of pseudomorphic structures has been used in literature for the explanation of extraordinary properties of late transition-metal (TM) submonolayers deposited on early TM surfaces<sup>7-9</sup>. Moreover, niobium pentoxide is an interesting promotor for several important catalytic processes<sup>10-12</sup>.

## EXPERIMENTAL

Experiments have been carried out in a stainless steel apparatus with a base pressure 10<sup>-8</sup> Pa, described elsewhere<sup>5</sup>, which was additionally equipped with a turbomolecular pump TPH 060 (Balzers, Liechtenstein). Detailed description of the sample preparation and of the TPD (TPR) measurements can be found in refs<sup>3,5</sup>. Partial pressures of the desorbed CO or CO<sub>2</sub> have been measured with a quadrupole mass spectrometer (MASSTORR DX, VG, U.K.) and throughout this work they were expressed in units of the output signal of the spectrometer, *viz.* in volts. The output signal has been plotted by an X-Y recorder. The recorded TPD curves were then for further analysis digitalized (without any additional smoothing procedure) by TechDig 1.1b software. This analysis comprised the peak areas estimation and fitting of the experimental curves by an optimized number of Gaussian functions.

The thickness of palladium layers has been followed by a thickness monitor, model IL 150 (Intellemetrics Ltd., U.K.). Palladium deposition parameters were: condensation temperature  $T_{\text{cond}} = 300$  K and the deposition rate  $r_{\text{dep}}$  was ranging between  $7 \times 10^{12}$  and  $17 \times 10^{12}$  atoms cm<sup>-2</sup> s<sup>-1</sup> (*cf.* ref.<sup>13</sup>). The heating rate of the sample during TPD measurements has been

$12 \text{ K s}^{-1}$ . Temperature range of TPD measurement was  $300 \leq T \leq 600 \text{ K}$ , because below  $T = 600 \text{ K}$  the investigated systems are stable<sup>4,8,9</sup>. Carbon monoxide layers have been prepared at  $\approx 305 \text{ K}$  by exposure of the sample surface to  $\approx 45 \text{ L}$  of CO (1 langmuir =  $1 \text{ L} = 1.33 \times 10^{-4} \text{ Pa s}$ ) ( $p_{\text{CO}} = 6.7 \times 10^{-7} \text{ Pa}$  for a time period of 120 s) which was expected to result in a full coverage of the palladium surface by CO (ref.<sup>3</sup>).

## RESULTS AND DISCUSSION

Carbon monoxide adsorption-desorption cycles on thin and thick palladium layers, deposited on a polycrystalline Nb foil, have been investigated. This comprised CO adsorption-desorption cycles on virgin Pd surfaces as well as repeated CO adsorption-desorption cycles. The results of these experiments were then compared with those obtained on palladium layers supported by an insulator interlayer ( $\text{Nb}_2\text{O}_5$  prepared by oxidation of the Nb foil<sup>3,5,6</sup> prior to palladium deposition).

At room temperature neither Nb nor  $\text{Nb}_2\text{O}_5$  surface was able to adsorb a significant amount of carbon monoxide without a palladium overlayer. Negligible desorption peaks on TPD curves were observed after the above defined standard CO exposure. Integrated areas of CO desorption peaks from mere Nb and  $\text{Nb}_2\text{O}_5$  surfaces, were two orders of magnitude lower than those observed with thinnest palladium layers.

Characteristic features of TPD curves (*i.e.* their shape, peak temperatures), obtained with carbon monoxide adsorbed at room temperature on a metal or oxide supported "virgin" palladium layers roughly corresponded to the published data even for Pd single crystal surfaces (Fig. 1, Table I). According to these results one can conclude that at least at room temperature the type of a support (metallic or oxidic) qualitatively does not influence chemisorption of carbon monoxide on a virgin palladium surface<sup>25</sup>. This does not hold, however, for the repeated adsorption-desorption measurements. A significant difference between the two investigated systems (Pd/Nb and Pd/ $\text{Nb}_2\text{O}_5$ /Nb) was observed after repeated CO adsorption (Fig. 2). Multiple states were detected on TPD curves after the second CO adsorption on thicker Pd layers (effective thickness  $d > 0.5 \text{ nm}$ ) in Pd/Nb systems, whereas only weakly bound CO species were observed on repeated TPD curves in the case of Pd/ $\text{Nb}_2\text{O}_5$ /Nb systems. No such a difference has been observed on thin palladium layers (effective thickness  $d \leq 0.5 \text{ nm}$ ). Since it is well known that atomically rough surfaces (high-index planes) usually exhibit a greater multiplicity of adsorption states than the flat surfaces<sup>26</sup>, one can tentatively propose that the observed effects are due to the differences in Pd-layers morphology.

Partial deactivation of Pd surfaces observed after the first TPD measurement (Fig. 2) could be, however, explained also by other factors. Besides healing out the defects, *i.e.* smoothening of the surface<sup>6</sup>, additionally following effects might be considered: (i) embedding of some Pd islands into the Nb oxide layer, (ii) formation of Pd–Nb bonds (eventually a surface alloy formation). All our experiments have been performed under the conditions<sup>4,6,9,14,27</sup>, preventing qualitative changes of neither the Pd/Nb nor

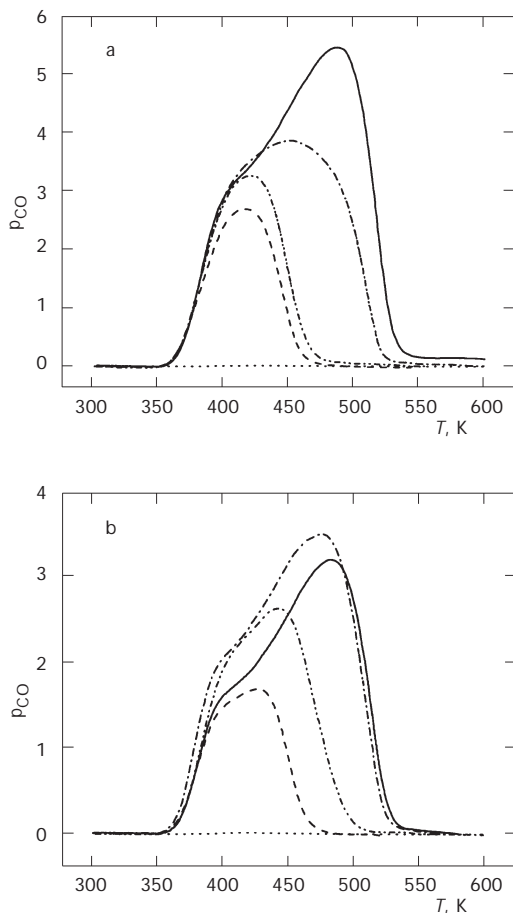


FIG. 1

TPD curves for the interaction of CO with Pd/Nb (a) and Pd/Nb<sub>2</sub>O<sub>5</sub>/Nb (b) surfaces. Values of the thickness of the outermost Pd layers for individual curves (in nm): ..... 0, - - - 0.3, - - - - 0.3, - - - - 0.85, - - - - 2.3 (a); .... 0, - - - 0.2, - - - - 0.5, - - - - 1.6, - - - - 2.3 (b). The output signal of the mass spectrometer expressed in V is used as a measure of the CO partial pressure  $p_{CO}$

Pd/Nb<sub>2</sub>O<sub>5</sub>/Nb system (diffusion of palladium into the oxidic or metallic support – Pd embedding or encapsulation, surface alloy formation). Moreover, the explanations sub (i) and sub (ii) can hardly elucidate the selective elimination of the most active Pd sites (coordinatively unsaturated palladium atoms at edges or corners of atomic steps). Consequently, the explanations sub (i) and sub (ii) have to be excluded. This, however, does not exclude the possibility of morphological changes in the palladium surface itself<sup>28</sup> (effect of Pd morphology changes).

Important role of morphological changes in the above described processes is supported by the observed effect of increasing the effective thickness of the palladium layer which results in an enhanced number of adsorbed CO molecules and of their fraction, bound more strongly to the sample surface (Fig. 1). The newly created active sites (coordinatively unsaturated edge and corner Pd atoms) appear on the surface after reaching a certain critical coverage<sup>28</sup> by growing 3D palladium islands<sup>6,12,27,29–32</sup>). Areas ( $A_0$ ) of CO desorption peaks (at the constant pumping speed proportional to the CO amount desorbed from a sample surface), resulting from CO ad-

TABLE I  
Carbon monoxide desorption from palladium samples

Pd sample	Low temperature shoulder, K	Peak temperature K	Reference
Pd/Nb	410	480	present study
Pd/Nb <sub>2</sub> O <sub>5</sub> /Nb	430	480	present study
Pd/Al <sub>2</sub> O <sub>3</sub>		480	14
Pd/Al <sub>2</sub> O <sub>3</sub>	370	470	15
Pd(320)(110)	390	480	16
Pd(110)	410	490	17
Pd(111)	420	470	18
Pd(110)	400	470	19
Pd/Mo		480	20
Pd (polycrystalline)	400	490	21
Pd(111)		490	22
Pd(polycrystalline)	400	500	23
Pd(100)	410	490	24

sorption on “virgin” sample surfaces, are presented in Fig. 3 as a function of the Pd-layer thickness. This quantity ( $A_0$ ) is used in next paragraphs as a measure of the Pd-layer surface area.

The decisive role of detailed morphology in the discussed phenomena is further supported by following experimental findings. The Pd/Nb samples in comparison with those of Pd/Nb<sub>2</sub>O<sub>5</sub>/Nb (of the same Pd-layer thickness):

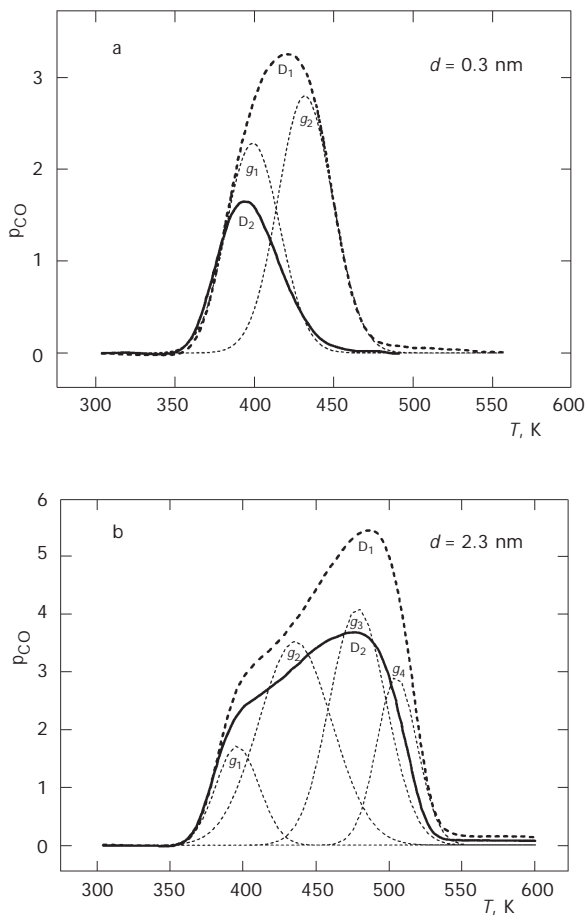


FIG. 2

TPD curves for CO desorption from thin and thick palladium layers of Pd/Nb (a, b) and Pd/Nb<sub>2</sub>O<sub>5</sub>/Nb (c, d) systems: thick dashed lines ( $D_1$ ) correspond to desorption after the first CO adsorption (thin dashed lines,  $g_i$  being its Gaussian components) and thick full lines ( $D_2$ ) correspond to the desorption after the repeated CO adsorption. Units of  $p_{CO}$  are defined in the same way as in Fig. 1 and  $d$  is the Pd-layer thickness

1. Exhibited always slightly higher values of peak temperatures ( $T_{\max}$ ) on the TPD curves, corresponding to a stronger adsorbate-adsorbent interaction on atomically rough surfaces. This is shown in Fig. 4, where the temperatures  $T_{\max}$  for Gaussian peaks (derived from fitting the experimental TPD curves by optimized number of Gaussian functions – examples are shown in Fig. 2) are plotted as a function of the palladium layer thickness ( $d$ ).

2. Exhibited always slightly higher values of a “specific” adsorbed amount of CO. Values of this quantity were obtained in the following way: individual Gaussian peak areas ( $a_i$ ) have been divided by the relevant values

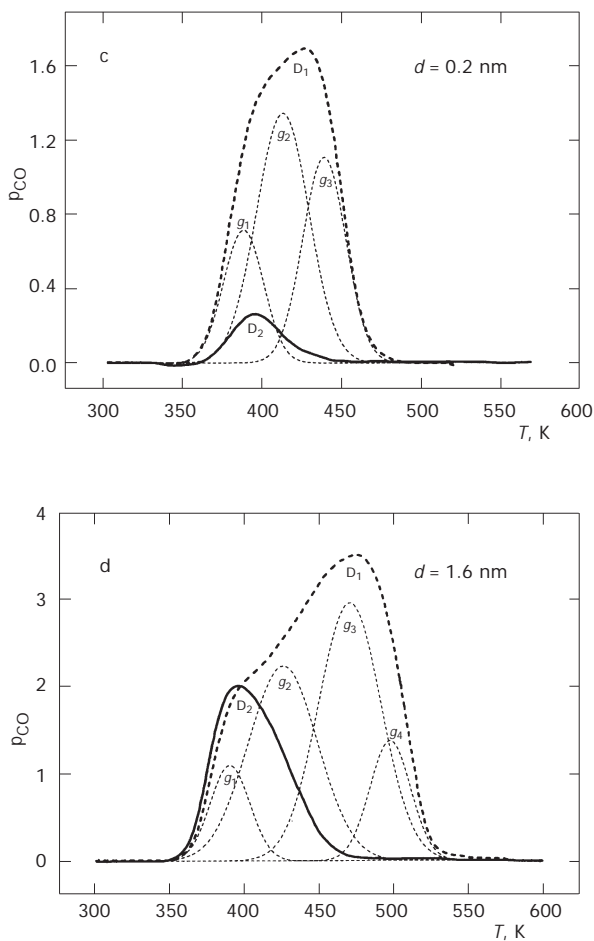


FIG. 2  
(Continued)

of  $A_0$  (for a given Pd-layer thickness  $d$  and for either Nb or  $\text{Nb}_2\text{O}_5/\text{Nb}$  supports). Figure 5 shows these “relative” Gaussian peak areas (expressed as a fraction of the desorbed CO amount after the “virgin” CO adsorption  $a_i/A_0$ )

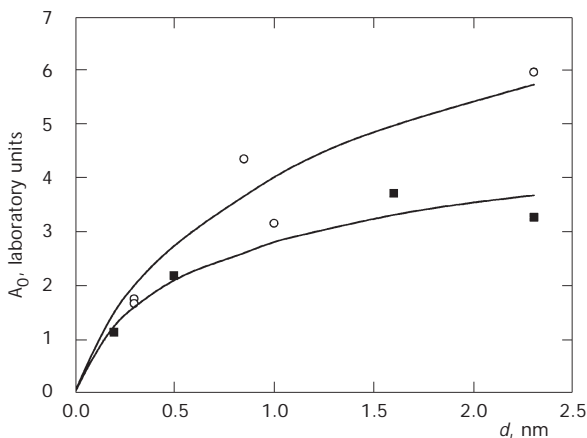


FIG. 3

Peak area  $A_0$  (resulting from CO adsorption on the “virgin” sample surface) plotted as a function of the thickness  $d$  of the Pd layer. Type of the support for individual experimental points: ○ Pd/Nb, ■ Pd/Nb<sub>2</sub>O<sub>5</sub>. Laboratory units are  $10^2$  V K

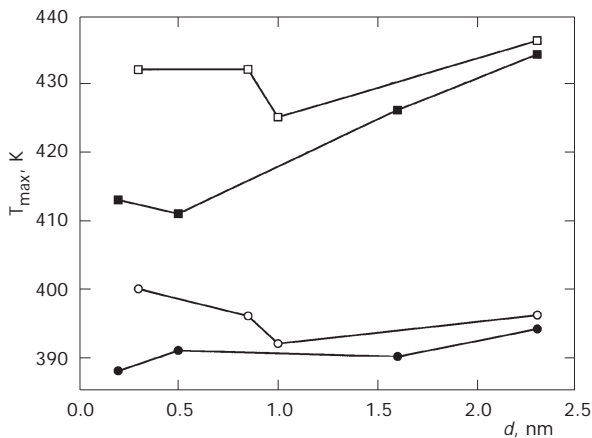


FIG. 4

Values of peak temperatures  $T_{\max}$  for Gaussian peaks (*cf.* Fig. 2) plotted as a function of Pd-layer thickness  $d$  for a metallic (Nb) and oxidic ( $\text{Nb}_2\text{O}_5$ ) support, derived from “virgin” TPD curves for CO. The individual points: ○ Pd/Nb, 1st Gaussian peak; □ Pd/Nb, 2nd Gaussian peak; ● Pd/Nb<sub>2</sub>O<sub>5</sub>, 1st Gaussian peak; ■ Pd/Nb<sub>2</sub>O<sub>5</sub>, 2nd Gaussian peak



plotted again as a function of the Pd-layer thickness. The above described procedure proved to be physically plausible as could be judged from the comparison of Fig. 5 with Fig. 6, where more or less randomly scattered absolute values of the Gaussian areas  $a_i$ , plotted as a function of  $d$ , were shown. Since high desorption peak temperatures  $T_{\max}$  are characteristic for

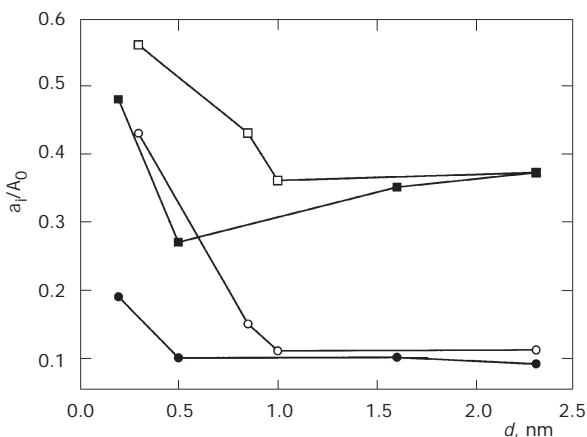


FIG. 5

“Relative” values of Gaussian peak areas  $a_i$  (for definition see the text) resulting from the “virgin” CO adsorption, are plotted as a function of Pd-layer thickness  $d$  for a metallic (Nb) and oxidic ( $\text{Nb}_2\text{O}_5$ ) support. The individual points as in Fig. 4

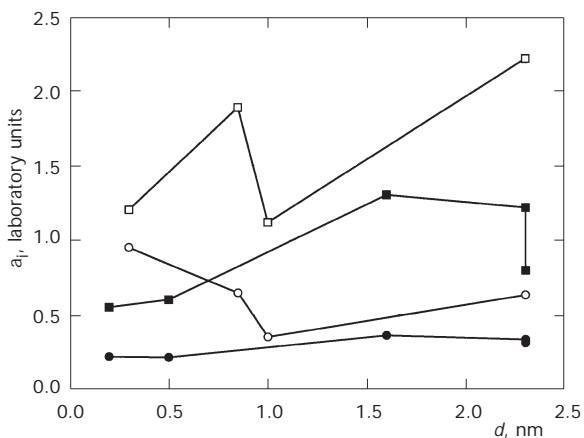


FIG. 6

Absolute values of Gaussian peak areas  $a_i$  plotted as a function of Pd-layer thickness  $d$  for the same systems as in Fig. 5. The individual points as in Fig. 4. Laboratory units are  $10^2 \text{ V K}$

atomically rough surfaces, exhibiting high surface areas, the ( $a_i/A_0$  vs  $d$ ) curves in Fig. 5 should correlate with Fig. 4 which is really the case. In agreement with general expectation, the values of  $T_{\max}$  (as well as values of  $a_i/A_0$ ) for both Pd/Nb and Pd/Nb<sub>2</sub>O<sub>5</sub>/Nb systems tend to converge at a higher Pd-layer thickness to a single  $T_{\max}$  (or  $a_i/A_0$ ) value (Figs 4 and 5).

Finally, since the heat treatment of the sample during the first TPD measurement obviously deactivates the most active sites (due to the smoothen-

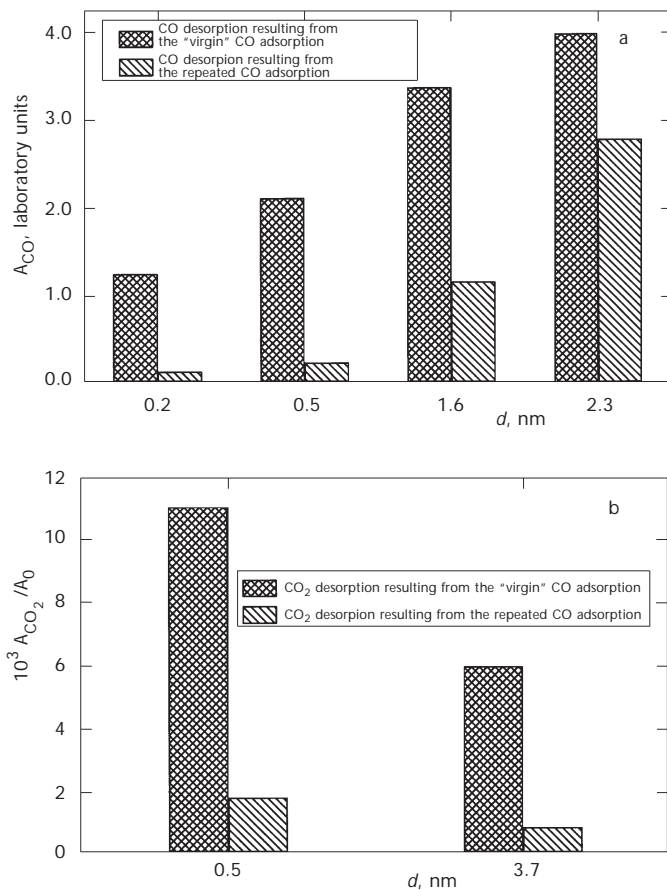


FIG. 7

Comparison of: absolute peak area values  $A_{\text{CO}}$  corresponding to amounts of CO desorbed from Pd/Nb<sub>2</sub>O<sub>5</sub>/Nb systems after the 1st and 2nd CO adsorption (a); relative values  $A_{\text{CO}_2}/A_0$ , corresponding to the amounts of CO desorbed from a Pd/Nb<sub>2</sub>O<sub>5</sub>/Nb system after the 1st and 2nd CO adsorption (b). The detailed specification can be found in the inset. Laboratory units are  $10^2$  V K

ing of the palladium surface<sup>28</sup>), naturally only less strongly bound species can be detected during the subsequent TPD measurement (Fig. 2d).

In addition to carbon monoxide, a small amount of carbon dioxide has been detected during the TPD of an adsorbed CO layer (Fig. 7). This CO<sub>2</sub> desorption results obviously from the disproportionation reaction  $2 \text{CO} \rightarrow \text{CO}_2 + \text{C}_{\text{ads}}$ . In comparison with CO desorption, the scale of desorbed amount of carbon dioxide is shifted towards lower values by about two orders of magnitude. Thus the experimental errors are naturally considerably higher than in the case of carbon monoxide. Consequently, any generalized conclusion is more or less unsafe in this case. CO<sub>2</sub> desorption from the adsorbed CO layer is considered to evidence a dissociated fraction of the adsorbed carbon monoxide<sup>33</sup>. Dissociative CO adsorption is expected to occur at the most active sites (edges of atomic layers, defects, *etc.*). The desorbed amount of CO<sub>2</sub> depends on the palladium thickness in Pd/Nb systems in a similar way to Pd/Nb<sub>2</sub>O<sub>5</sub>/Nb systems (Fig. 8). The shape of the obtained ( $A_{\text{CO}_2}$  vs  $d$ ) curves is qualitatively identical; however, they differ quantitatively. This could be understood to be due again to morphological rather than to chemical differences between the two systems. This conclusion is supported also by results presented in Fig. 9 which shows the “relative decrease” in the desorbed amounts of CO between the 1st and 2nd or 3rd adsorption–desorption cycles. These “relative CO amounts” are expressed in terms of peak-area differences  $^1A_{\text{CO}} - ^2A_{\text{CO}}$  and  $^1A_{\text{CO}} - ^3A_{\text{CO}}$ , respectively,

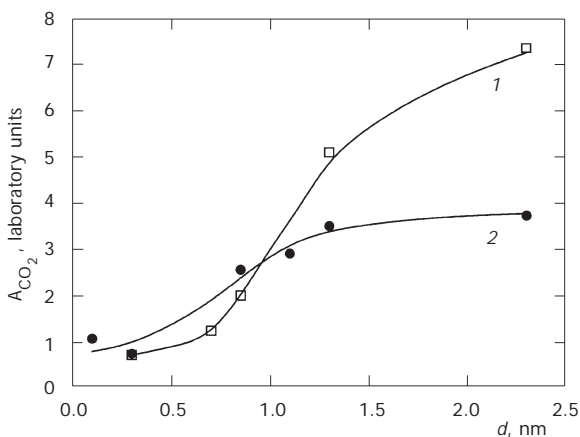


FIG. 8

Influence of the Pd-layer thickness on the values of peak areas of CO<sub>2</sub>  $A_{\text{CO}_2}$ , desorbed from Pd/Nb (1,  $\square$ ) and Pd/Nb<sub>2</sub>O<sub>5</sub>/Nb (2,  $\bullet$ ) systems plotted as a function of Pd-layer thickness  $d$

divided by the relevant  $A_0$  ( ${}^2A_{\text{CO}} \approx {}^3A_{\text{CO}}$ ). These data seem to fall, within experimental errors, onto a single curve (Fig. 8).

Under the experimental conditions used in this investigation (deposition of submonolayers and thicker layers of palladium at room temperature in a UHV system onto clean and oxidized Nb surfaces, temperature range 300–600 K used in TPD), it seems to be well proved that the type of the support influences mainly the morphology of the active metal (Pd) layer. This means in our case that the palladium layers, deposited on a metallic Nb surface, exhibit larger roughness than those deposited on  $\text{Nb}_2\text{O}_5/\text{Nb}$  substrates. One can ask then about the physical basis of this phenomenon.

There are several macroscopic factors influencing the initial growth and thus also the resulting final morphology of the evaporated thin layers, *e.g.* temperature and chemical nature of the support, deposition rate and direction of impinging particles. From the point of view of a molecular mechanism of the Pd layer growth there are two types of decisive factors: thermodynamic factors (*e.g.* Pd–Pd, Pd–Nb and Pd– $\text{Nb}_2\text{O}_5$  bond energy) and kinetic ones (*e.g.* dissipation of excess kinetic energy of Pd atoms in relation to the activation energy of their surface migration). On the basis of the presented results it is believed that in this case the kinetic factors play the most important role. Switching from a metallic to an oxidic condensation surface changes (among other conditions) the efficiency of the excess ki-

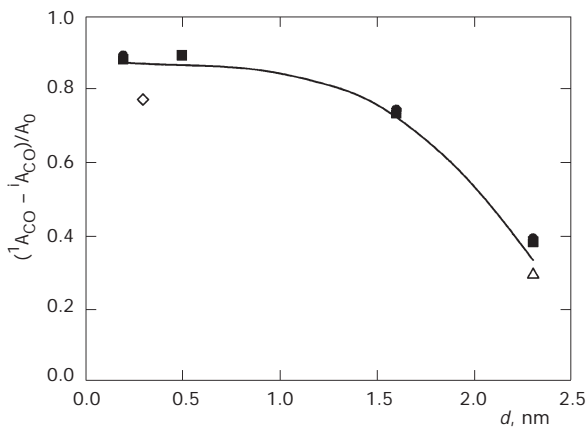


FIG. 9

“Relative” decrease in the peak area corresponding to the CO amount desorbed during the 1st ( ${}^1A_{\text{CO}}$ ), 2nd ( ${}^2A_{\text{CO}}$ ) and 3rd ( ${}^3A_{\text{CO}}$ ) adsorption-desorption cycle. Individual points: ◇ ( ${}^1A_{\text{CO}} - {}^2A_{\text{CO}}/A_0$ ) (Pd/Nb), △ ( ${}^1A_{\text{CO}} - {}^3A_{\text{CO}}/A_0$ ) (Pd/Nb), ■ ( ${}^1A_{\text{CO}} - {}^2A_{\text{CO}}/A_0$ ) (Pd/ $\text{Nb}_2\text{O}_5$ ), ● ( ${}^1A_{\text{CO}} - {}^3A_{\text{CO}}/A_0$ ) (Pd/ $\text{Nb}_2\text{O}_5$ )

netic energy dissipation of the Pd atoms. In the case of an oxide surface, a less efficient energy dissipation can be expected because of large difference of masses of the impinging metal atoms and target particles in the surface. The “hot” metal atoms can then migrate along the surface to favorable sites (deepest potential energy wells). Thus a less defective surface (smooth on the atomic scale) can be expected to be formed. On the other hand, in the case of a metallic support, the excess energy dissipation is more efficient, because of favorable mass ratio. Moreover, there are additional dissipation channels on the metallic support surface (plasmon creation, electron-hole pair creation, *etc.*). Consequently, atomically rough surfaces can be expected to grow on metallic supports. Therefore, the active metal layers (in this case Pd layers deposited on metallic Nb surface) exhibit higher desorption-peak temperatures  $T_{\max}$  and larger amounts of CO and CO<sub>2</sub> desorbed from a unit surface area.

The values of desorption peak temperatures ( $T_{\max}$ ) can be used for an approximate estimation of the desorption activation energies<sup>34</sup>. The limiting value of the carbon monoxide desorption-peak temperature was in our experiments  $T_{\max} = 480$  K. According to ref.<sup>34</sup>,  $E_d^{\text{monox}} \approx 0.0025 T_{\max} [\text{eV}] = 115 \text{ kJ mol}^{-1}$ , which roughly corresponds to the published data (published values for CO desorption from: (i) Pd/Al<sub>2</sub>O<sub>3</sub>/NiAl  $E_d^{\text{monox}} = 136 \pm 9 \text{ kJ mol}^{-1}$  (ref.<sup>13</sup>), (ii) Pd/TiO<sub>2</sub>  $E_d^{\text{monox}} = 135 \text{ kJ mol}^{-1}$  (ref.<sup>35</sup>). Similarly, the limiting peak temperature for carbon dioxide desorption was  $T_{\max} = 420$  K, corresponding to  $E_d \approx 96 \text{ kJ mol}^{-1}$ . Since CO<sub>2</sub> is extremely weakly adsorbed on

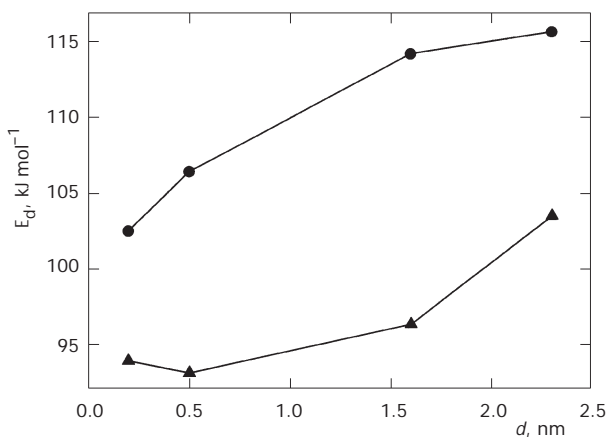


FIG. 10

Activation energies for the 1st (●) and 2nd (▲) CO adsorption-desorption cycles plotted as a function of Pd-layer thickness  $d$

platinum group metals<sup>36,37</sup> the life-time of the newly formed CO<sub>2</sub> molecule is immeasurably short<sup>37</sup>. Therefore, the obtained  $E_d = 96 \text{ kJ mol}^{-1}$  should be identified most probably with the activation energy of the surface reaction producing CO<sub>2</sub> (surface reaction of dissociated species) in a good agreement with literature (published values of activation energies of the surface reaction  $\text{CO}_{\text{ads}} + \text{O}_{\text{ads}} \rightarrow \text{CO}_2$  are: (i) for the Pd/Al<sub>2</sub>O<sub>3</sub>/NiAl system  $E = 60 \text{ kJ mol}^{-1}$  (ref.<sup>36</sup>), (ii) for Pd (111)  $E = 100 \text{ kJ mol}^{-1}$  (ref.<sup>38</sup>). (Note: The Pd islands supported by Al<sub>2</sub>O<sub>3</sub> expose in the gas phase mainly (111) crystallographic layers<sup>13,36</sup>.)

The desorption activation energies, calculated for the first and second CO adsorption–desorption cycles, respectively, are shown in Fig. 10, illustrating the previous qualitative statement, concerning the “reversible” part of the CO adsorption on a Pd/Nb<sub>2</sub>O<sub>5</sub>/Nb system (Fig. 2).

## CONCLUSIONS

1. The observed discrepancy between the first (“virgin”) and subsequent TPD measurements in systems CO–Pd/Nb and CO–Pd/Nb<sub>2</sub>O<sub>5</sub>/Nb can be understood in terms of morphological differences between the two Pd layers deposited on different supports, rather than in terms of electronic Pd–Nb interaction or palladium embedding into the support material.

2. The kinetic factors seem to play a dominant role in the formation of the final shape of the Pd-layer surface.

3. Approximate values of activation energies for the CO desorption and CO<sub>2</sub> formation in the disproportionation reaction were estimated by an empirical method<sup>34</sup>. These values were in a reasonable agreement with relevant published data.

*The support of this work by the Grant Agency of the Czech Republic (grants No. 202/98/K002 and No. 202/02/0618) is gratefully acknowledged. The authors appreciate assistance of Mr M. Werner, M.S. in construction of experimental equipment and the technical assistance of Ms M. Knapová in preparation of this manuscript.*

## REFERENCES

1. Rumpf F., Poppa H., Boudart M.: *Langmuir* **1988**, 4, 722.
2. Bowker M., Bowker L. J., Bennett R. A., Bennett R. A., Stone P., Ramirez-Cuesta A.: *J. Mol. Catal., A* **2000**, 163, 221.
3. Jirsák T., Nikolajenko V., Knor Z.: *J. Phys. Chem.* **1995**, 99, 15470.

4. Thiam M. M., Bastl Z.: *Surf. Sci.* **2002**, *507*, 678.
5. Jirsák T., Nikolajenko V., Knor Z.: *Collect. Czech. Chem. Commun.* **1994**, *59*, 1709.
6. Jirsák T., Nikolajenko V., Knor Z.: *Collect. Czech. Chem. Commun.* **1997**, *62*, 575.
7. El-Batanouny M., Hamann D. R., Chubb S. R., Davenport J. W.: *Phys. Rev. B: Condens. Matter* **1983**, *27*, 2575.
8. Ruckman M. W., Strongin M.: *Am. Chem. Res.* **1994**, *27*, 250.
9. Selidj A., Koel B. E.: *Surf. Sci.* **1993**, *281*, 223.
10. Ziolk M.: *Catal. Today* **2003**, *78*, 47.
11. Tanabe K.: *Catal. Today* **2003**, *78*, 65.
12. Noronha F. B., Aranda D. A. G., Ordine A. P., Schmal M.: *Catal. Today* **2000**, *57*, 575.
13. Libuda J., Meusel I., Hoffmann J., Hartmann J., Piccolo L., Henry C. R., Freund H.-J.: *J. Chem. Phys.* **2001**, *114*, 4669.
14. Shaikhutdinov Sh., Heemeier M., Hoffmann J., Meusel I., Richter B., Bäumer H., Kühlenbeck H., Libuda J., Freund H.-J., Oldman R., Jackson S. D., Konvicka C., Schmid M., Varga P.: *Surf. Sci.* **2002**, *501*, 270.
15. Matolín V., Stará I., Tsud N., Johánek V.: *Prog. Surf. Sci.* **2001**, *67*, 167.
16. Hirsimäki M., Valden M.: *J. Chem. Phys.* **2001**, *114*, 2345.
17. Yagi-Watanabe K., Fukutani H.: *J. Chem. Phys.* **2000**, *112*, 7652.
18. Carrez S., Dragnea B., Zheng W. Q., Dubost H., Bourguignon B.: *Surf. Sci.* **1999**, *440*, 151.
19. Jones I. Z., Bennett R. A., Bowker M.: *Surf. Sci.* **1999**, *439*, 235.
20. Xu Ch., Goodman D. W.: *Surf. Sci.* **1996**, *360*, 249.
21. Matolín V., Rebholz M., Kruse N.: *Surf. Sci.* **1991**, *245*, 233.
22. Guo X., Yates J. T., Jr.: *J. Chem. Phys.* **1989**, *90*, 6761.
23. van Hieu N., Craig J. H.: *Surf. Sci.* **1984**, *145*, L493.
24. Behm R. J., Christmann K., Ertl G., van Hove M. A.: *J. Chem. Phys.* **1980**, *73*, 2984.
25. Giorgi J. B., Schroeder T., Bäumer H., Freund H.-J.: *Surf. Sci.* **2002**, *498*, L71.
26. Christmann K.: *Introduction to Surface Physical Chemistry*. Steinkopf-Verlag, Darmstadt and Springer-Verlag, New York 1991.
27. Heemeier M., Stempel S., Shaitkhitdinov Sh. K., Libuda J., Bäumer H., Freund H.-J.: *Surf. Sci.* **2003**, *523*, 103.
28. Beck D. E., Heitzinger J. H., Avoyan A., Koel B. E.: *Surf. Sci.* **2001**, *491*, 48.
29. Campbell C. T.: *Surf. Sci. Rep.* **1997**, *27*, 1.
30. Wolter K., Seifert O., Kühlenbeck H., Bäumer M., Freund H.-J.: *Surf. Sci.* **1988**, *399*, 190.
31. Xu C., Goodman D. W.: *Surf. Sci.* **1996**, *360*, 249.
32. Suzuki T., Souda R.: *Surf. Sci.* **2000**, *448*, 33.
33. Johánek V., Stará I., Tsud M., Veltruská K., Matolín V.: *Appl. Surf. Sci.* **2000**, *162–163*, 679.
34. Knor Z.: *Surf. Sci.* **1985**, *154*, 2233.
35. Bowker M., Stone P., Bennett R., Perkins N.: *Surf. Sci.* **2002**, *497*, 155.
36. Hoffmann J., Schaueremann S., Hartmann J., Zhdanov V. P., Kasemo B., Libuda J., Freund H.-J.: *Chem. Phys. Lett.* **2002**, *354*, 403.
37. Ertl G. in: *Catalysis: Science and Technology* (J. R. Anderson and M. Boudart, Eds), Vol. 4. Springer-Verlag, Berlin 1984.
38. Engel T., Ertl G.: *J. Chem. Phys.* **1978**, *69*, 1267.